COVER SHEET

Paper Number: **1820**

TITLE: **MODELING OF RESIN TRANSFER MOLDING OF CARBON FIBER COMPOSITES**

Authors: Venkat Aitharaju[*]
Hang Yu[$]
Selina Zhao[*]
John Owens[*]
Praveen Pasupuleti[$]
Mark Doroudian[$]

ABSTRACT

Resin transfer molding (RTM) has become increasingly popular for the manufacturing of composite parts. To enable high volume manufacturing and obtain good quality parts at an acceptable cost to automotive industry, accurate process simulation tools are necessary to optimize the process conditions. Towards that goal, General Motors and the ESI-group are involved in developing a state of the art process simulation tool for composite manufacturing in a project supported by the Department of Energy. This paper describes the modeling of various stages in resin transfer molding such as resin injection, resin curing, and part distortion. An instrumented RTM system located at the General Motors Research and Development center was used to perform flat plaque molding experiments. The experimental measurements of fill time, in-mold pressure versus time, cure variation with time, and part deformation were compared with the model predictions and very good correlations were observed.

INTRODUCTION

Resin transfer molding (RTM) has recently come into prominence as a high-speed, high-volume process for the manufacturing of automotive components at a higher through-put and lower cost compared to traditional methods [1,2]. In the RTM process, a dry preform is first draped onto the mold, the mold is closed, and then a low viscosity resin is injected into the mold under pressure. In an RTM process, there are three significant stages in molding; a) resin injection (filling) b) resin curing and c) part ejection and cooling. Injection is the stage where the resin is injected into the mold cavity with the fiber preform to make sure that resin wets out the fibers. After the resin fills the mold cavity, the injection is stopped. A curing agent is added to the resin prior to the resin injection to accelerate the curing process. Curing is the stage when the resin polymerizes and becomes solid around the fibers.

Venkat Aitharaju[*], Selina Zhao[*], John Owens[*], General Motors LLC, 30500 Mound Rd, Warren, MI - 48092, U.S.A..
Hang Yu[$] , Praveen Pasupuleti[$], Mark Doroudian [$], ESI Group, North America, Farmington Hills, MI, 48334

The time for curing is a very important element in determining the total manufacturing time/throughput of a part. Recent development of fast curing resins have significantly reduced cure times, directly reducing cycle time. After making sure that sufficient cure has taken place for the part in the mold, the part is removed from the mold and allowed to cool. During the cooling stage, the part may experience significant residual stresses causing the part to warp. There are several challenges associated with resin transfer molding and they are: adequate wetting of fibers with no voids in the part during the injection, minimizing the fill time by optimizing the number of gates and gate locations, optimize the hold time for the part inside the mold to allow adequate curing, and the part meeting the dimensional requirements for the assembly. Accurate simulation capability to address the above mentioned challenges upfront during the design stage and eliminate the trial and error is the key to potentially use the RTM process for high volume automotive manufacturing.

Bickerton and Advani [3] conducted several experiments to develop a library of isothermal experimental flow visualizations and pressure measurement data to validate the numerical simulations. Experiments were performed to study the change in the volume fraction of the preform with injection pressure, and the effect of racetracking on the fill time in the injection stage were investigated and correlated with numerical simulations. A good agreement between the numerical predictions and the experimental results were observed. A finite element program called RTMSIM [4] was developed at University of California at Los Angles (UCLA) to model the resin transfer molding using an implicit time integration algorithm. The model assumed isothermal flow injection. The developed code RTMSIM has been validated by comparing its predictions with closed-form solutions for flat plates. The code was also shown to deal with capillary pressure for conducting a wicking analysis. Tari, et.al [5] conducted the two-dimensional flow field study during the resin transfer molding using the computer program RTMSIM and showed that adding a highly permeable layer to the preform can decrease the fill time significantly. Mohan et.al [6] developed a finite element model to solve for the pressure and fill factors for tracking the flow front iteratively using implicit framework. Several complex geometrical mold shapes were tried to demonstrate the applicability to practical manufacturing process simulations. The implicit frame works was shown to be 30 times faster than the traditional explicit finite element-control volume approach. Lee, et.al [7], based on computer simulations, proposed a method to detect and prevent defects originating from random variation of permeability and microscopic non-uniformity. They propose a real-time control of void formation by manipulating the auxiliary gates closer to the flow front. Nguyen, et. al [8] developed a model for the natural fiber reinforcement considering diameter increase with resin infusion and time dependent permeability change with fiber diameter increase. The developed model was able to predict results close to experiments compared to commercial programs. Bhat et.al [9] conducted a parametric analysis of the process parameters effecting the filling time in compression resin transfer molding using the LIMS software being developed at University of Delaware. They observed that as the stiffness of the preform is increased, the fill time also increases.

Curing process was simulated by several researchers using elastic and viscoelastic models. Wang et. al [10] studied curing process-induced internal stress

and deformation of carbon fiber/epoxy composites using both elastic and viscoelastic models. Based on the numerical results obtained, they concluded that difference between the results reduce as the fiber volume fraction increased and the value of the resin shrinkage decreased. Adolf and Martin [11] developed a general constitutive model for calculating the evolution of stresses in thermoset systems. They assumed the total strain to be finite such that linear viscoelasticity applies. Using the developed model, various ways of minimizing the cure stresses through control of the cure cycle was studied. Eom, et. al [12] described the evolution of relaxation modulus of an epoxy-amine system during the cure and at any cure temperature with a phenomenological model. A time-cure-temperature superposition concept was introduced in their work. This model was shown to predict the viscoelastic stress build-up following any industrial cure cycle. Excellent agreement was observed between the experimental and the numerical predictions. Svanberg and Holberg [13] studied experimentally the effect of cure schedule in spring-in mechanism of glass fiber composites. Significant contribution from each of three mechanisms, namely different thermal expansion in glassy and rubbery state, chemical shrinkage and froze-in deformation caused by constrained in-mold cure were studied. Shi and Dong [14], using the unstructured tetrahedron mesh, conducted numerical simulation for 3D non-isothermal RTM process accounting for Darcy's fluid flow, heat transfer and curing kinetics. The mesh was shown to have good adaptability to complex part shapes and complicated flow field than structured finite element mesh. A good agreement between the numerical and experimental results was obtained. Delegalized et. al [15] studied the highly reactive resin with short curing cycle. The resin viscosity was considered as function of temperature, cure and also time. The developed algorithm were shown promising to implement in the commercial numerical simulation software. Ruiz and Trochu [16] developed a reaction kinetic model for the resin, mechanical property model to predict properties as function of polymerization and glass transition temperature. A classical laminate theory was applied to calculate the internal stresses and thus predict warpage. An optimization algorithm was applied to demonstrate the reduction of warpage by transient heating and cooling of the part.

One can see from the above literature study that several researchers have developed modeling schemes to cater for the three stages of resin transfer molding. However, very few efforts deal with numerical aspects of all the stages of the RTM process. In the present study, the RTM process was studied in the framework of PAM-RTM and PAM-DISTORTION computer programs for all the stages. Molding experiments were conducted using an instrumented RTM system available in General Motors Laboratories. Material characterization tests were performed for the resin viscosity to provide the data for simulation. Simulations were conducted for the three stages of RTM process and the results from the simulations are compared with the experimental results for validation. In the following sections, details about the mathematical approach for modeling of various stages of RTM, description of the preform, experiments performed for generating the data, validation of the numerical simulations by comparing with the experimental results, are followed by brief conclusions.

MODELING APPROACH

There are four physical phenomena that need to be modeled in the resin transfer molding. They are namely, a) the resin flow through the porous media, b) the thermal heat transfer between the resin, fiber, and the mold, c) the chemical reaction in the curing process, and d) the residual stresses during the cooling of the part.

The flow of the resin is assumed to be governed by the Darcy's law, which states that the flow rate of the resin per unit area (velocity) is directly proportional to the pressure gradient and inversely proportional to the viscosity of the resin. The constant of proportionality is called the permeability of the porous medium.

$$V = -\frac{K}{\mu}\nabla P \tag{1}$$

According to the conservation of mass, the velocity field needs to satisfy (with constant density assumption):

$$\nabla \cdot V = 0 \tag{2}$$

By combining the equations (1) and (2), we get

$$\nabla \cdot (-\frac{K}{\mu}\nabla \mathrm{P}) = 0 \tag{3}$$

The viscosity of the thermoset epoxy resin is typically dependent on the temperature, and the approximation of the dependence is described by the following model:

$$\mu(T) = a(\frac{1}{\mathrm{T}})^{\mathrm{b}} \tag{4}$$

where T is the temperature, a, b are the fitting parameters based on viscosity calibration data.

The temperature filed is governed by the following equation [25]:

$$\rho C_p \frac{\partial T}{\partial t} + \rho_r C_{pr} V \cdot \nabla T = \nabla \cdot (k \cdot \nabla T) - \rho_r \Delta h \frac{d\alpha}{dt} \tag{5}$$

where T again denotes the temperature, t is the time, ρ is the density, C_p is the specific heat, k is the thermal conductivity tensor, the subscript r designates the resin, Δh is the total enthalpy of the polymerization of the resin, α is the degree of cure of the resin.

During the injection simulation, following effective properties for the heat capacity and permeability were used:

For non-impregnated fibers:

$$\rho C_p = \emptyset \rho_a C_{pa} + (1 - \emptyset)\rho_f C_{pf} \tag{6}$$

$$k = \emptyset k_a + (1 - \emptyset)k_f \tag{7}$$

For impregnated fibers:

$$\rho C_p = \emptyset \rho_r C_{pr} + (1 - \emptyset)\rho_f C_{pf} \quad (8)$$

$$k = \emptyset k_r + (1 - \emptyset)k_f \quad (9)$$

Where the subscript r denotes the resin, f indicates the fibers a denotes the air, and $\emptyset$ is the porosity of the preform. In general, we can neglect the thermal properties of the air.

The differential equation (5) was solved using an implicit solver available in PAM-RTM computer program. An adaptive time step was used to solve the equations incrementally. The time step size was chosen to ensure the stability of the solution for flow, thermal and cure problem.

The degree of cure of the resin can described by using Kamal-Sourour model [17] and is given by:

$$\frac{d\alpha}{dt} = (A_1 \exp\left(-\frac{E_1}{T}\right) + A_2 \exp\left(-\frac{E_2}{T}\right) \cdot \alpha^m) \cdot (B - \alpha)^n \quad (10)$$

where A_i are the rate constants with an Arrhenius type of dependence with temperature, E_i are the energies of activation of the chemical reaction, and m and n are exponents characterizing the sensitivity of each autocatalytic reaction. The value of B for many resin types was assumed as 1.0.

The distortion simulation model is based on the model proposed by Svanberg [18] which was implemented in Pam-Distortion computer program. The model was derived based on the assumption of linear viscoelasticity for the resin and the rate dependency was replaced by a path dependence on the state variables such as strain, degree of cure, and the temperature. Two types of strains were considered, mostly from thermal expansion and chemical shrinkage due to the crosslinking reaction and finally the frozen-in deformation in the mold. In the present work, the residual stress were calculated taking into account the phase change of the resin during curing. Initially the resin is liquid and sustains no strain or stress during the curing. As the curing progresses, the macromolecular network becomes infinite and the resin starts to become rubbery and starts to resist the stresses. The degree of cure at which resin changes the state from liquid to rubbery is called as gelation. The degree of cure at gelation is an important parameter and can be measured by conducting isothermal experiments for viscosity. At gelation, one can observe a steep increase in viscosity. Further, as the curing continued and when the temperature of the resin reaches the glass transition temperature of the resin, the resin is said to be in a glassy state.

The glass transition temperature evolution with curing degree was described using Di Benedetto model [19] and is given below:

$$\frac{T_g - T_{g0}}{T_{g\infty} - T_{g0}} = \frac{\lambda\alpha}{1-(1-\lambda)\alpha} \quad (11)$$

Where T_{g0} is the glass transition temperature of the uncured system ($\alpha = 0$), $T_{g\infty}$ is the glass transition temperature of the fully cured system ($\alpha = 1$), and λ is a material constant measured from the experiments.

Carbon Fiber Preform

Dry non-crimp fabric (NCF) carbon fiber materials procured from Sigmatex were used in the as preform for molding experiments. The four layer NCF preform has the nomenclature Non-Crimp (Sigmatex BMC933 1270mm-50" / T700SC 12K product # MC9331270). The preform fabric was multi-oriented (0/+45/-45/90). Two layers of such preform were used to form a symmetric preform (0/45/-45/90/90/-45/45/0). Square preforms were cut with exact mold dimensions and placed to eliminate any racetracking on the sides.

EXPERIMENTAL METHOD

A small, custom-built RTM apparatus available in General Motors Research Labs was used for the molding experiments. The RTM apparatus is a two-stream machine that uses hydraulic cylinders to pump the resin and the curing agent. Precise control of flow rates is achieved via computer controlled pumping of hydraulic oil with gear pumps. Linear Variable Distance Transducers (LVDT's) are used to measure the displacement of the cylinder pistons thereby monitoring the volume of resin pumped. Figure 1 shows a schematic of the apparatus.

The cylinders and flex lines for each component are individually jacketed with heating tape enabling temperature control of both streams. The GM RTM system is capable of delivering a pre-heated, mixed resin to a mold at up to 250 PSI (1.72 MPa) with flow rates up to 50 cc/sec. An instrumented plaque mold was designed for use with the RTM apparatus. This mold cavity is 17.5 inches long, 17.5 inches wide, and 0.12 inches thick. Opposing, centered end gates are used for the inlet and vent ports of the mold. Three flush mounted dielectric cure sensors and three flush mounted pressure transducers are positioned in the top half of the mold. Their locations are along the centerline of the mold near the inlet, at the midpoint, and near the vent. Thermocouples are integrated into the dielectric cells and additional thermocouple ports are located near each of the four corners of the mold. Figure 2 shows the mold design. With the flow rate control available from the GM RTM apparatus, fill times as short as 10 seconds and as long as 60 seconds can be attained. A data acquisition computer controls the RTM experiment and records the LVDT signals, pressures, and temperatures. The dielectric cure data is collected via a Lambient Dielectric Cure system running on a second computer.

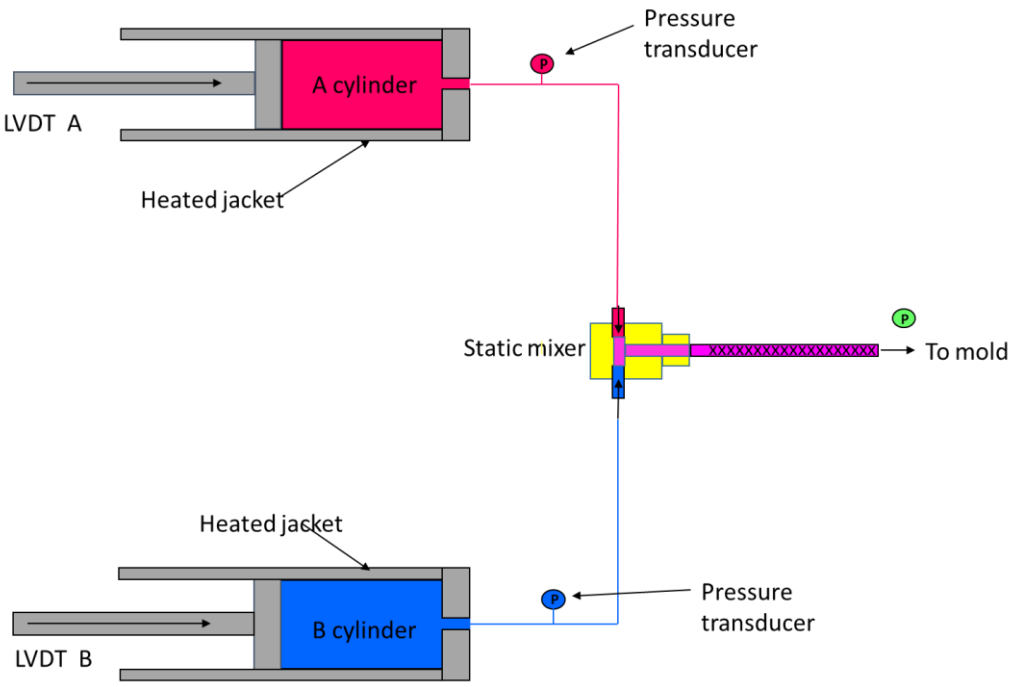

Figure 1. Schematic of GM research two-stream RTM

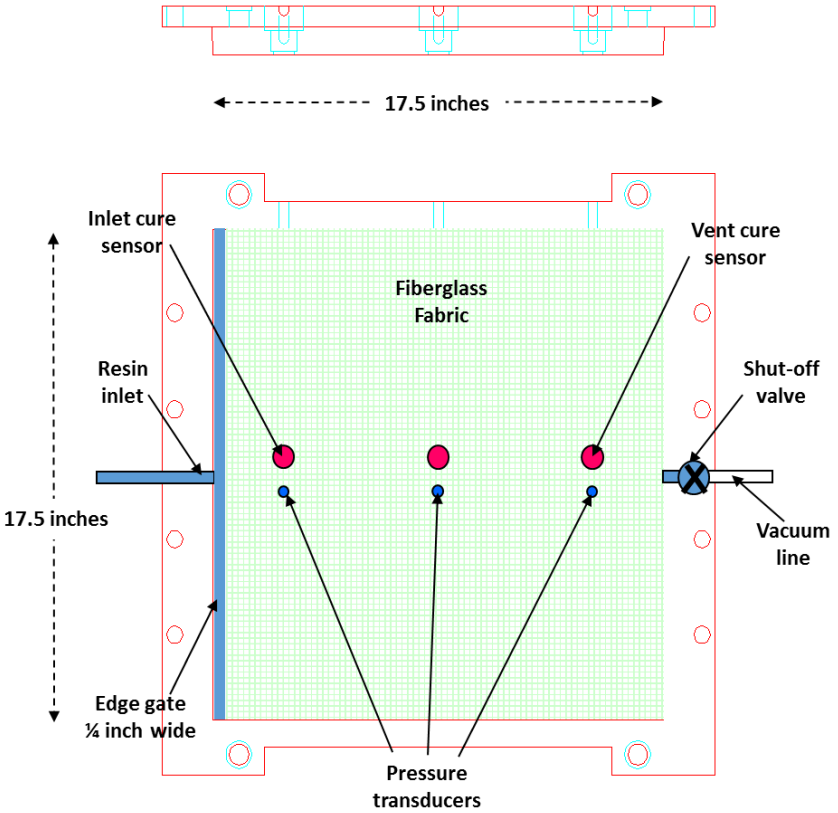

Figure 2. Instrumented Plaque Mold for RTM

Table I: RTM epoxy resin formulation

Component	Source	Formulation amount
Epoxy resin	Dow 383	100
Anhydride (MTHPA)	Lonza (now Broadview Chemical)	80
Catalyst (t-butyl ammonium Br)	Aldrich	3

With the objective of facilitating computer simulations of RTM molding, a well characterized epoxy resin system was selected. The RTM resin chosen consists of a low cost, general purpose DGEBA epoxy resin and a low viscosity anhydride curing agent. This system requires a catalyst to enable short cure times. With the limitation of the two stream RTM apparatus, the catalyst must be soluble and stable in either the epoxy resin or the anhydride. For this resin, a quaternary ammonium salt was chosen as the catalyst because it could be safely dissolved into the epoxy resin stream at a 3% loading. The resin formulation is provided in Table I.

Resin viscosity as a function of temperature was previously measured for this system. These viscosity measurements were carried out by omitting the catalyst from the formulation in order to allow sufficient time to take data before the curing reaction gets started. The viscosity versus temperature data measured from the experiments for the chosen RTM resin is presented in Figure 3.

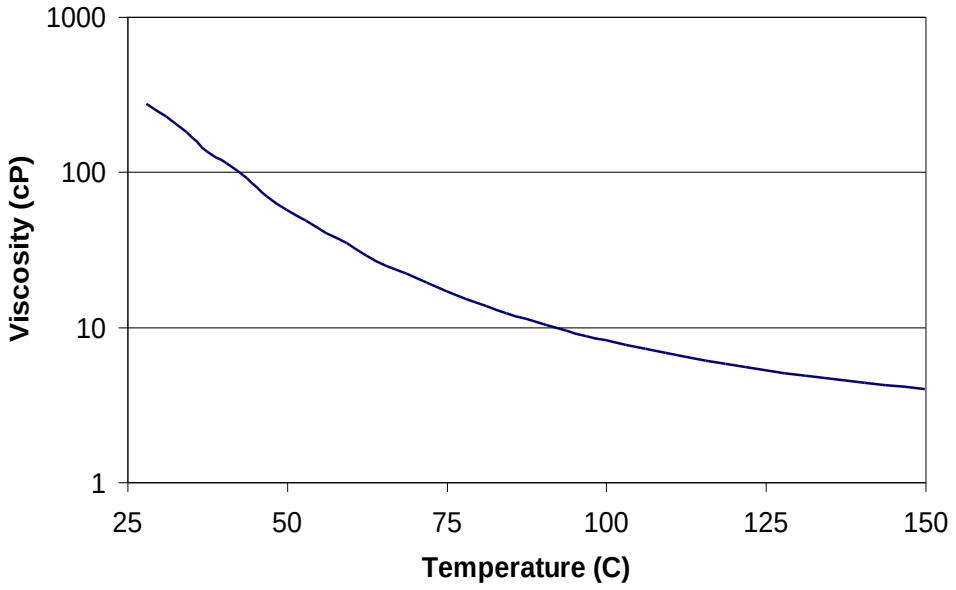

Figure 3: Viscosity vs Temperature for the Epoxy / MTHPA Resin System

Development of Kinetics Model For The Curing Analysis:

In this work, a set of seven constant heating rate DSC experiments were performed on the epoxy resin system. Isothermal DSC experiments can also be used, but analysis of the data is made difficult by the inevitable curing that can take place during the rapid heating up to the isothermal temperature. Due to this difficulty, we have found better results using constant heating rate experiments with heating rates ranging from 2^0 C/min to 20^0 C/min.

The chemical rate kinetic model fitting was performed using the PolyKinetic software program developed and written at Ecole Polytechnique de Montreal. For this work, the Kamal-Sourour kinetic model [17] was chosen. This model is an empirical model that has been found to yield reasonably accurate models for a large number of epoxy based resin systems. Although an empirical model with six parameters, it is based on autocatalytic mathematics that can reproduce an apparent induction time followed by an accelerating cure rate. The PolyKinetic software uses a least-square Levenberg-Marquardt nonlinear regression algorithm for the calculation of the unknown parameters of the kinetic models. As evidenced by the above Figure 4, the optimized parameters give a reasonable accurate prediction of reaction rates over a wide range of temperature and degree of cure. The model parameters for Kamal-Sorour model are given by:

$$\frac{d\alpha}{dt} = (0.1179e^{-\frac{4117}{T}} + 3.32E6 * e^{-\frac{7836.3}{T}}\alpha^{0.457})(1-\alpha)^{1.199} \qquad (12)$$

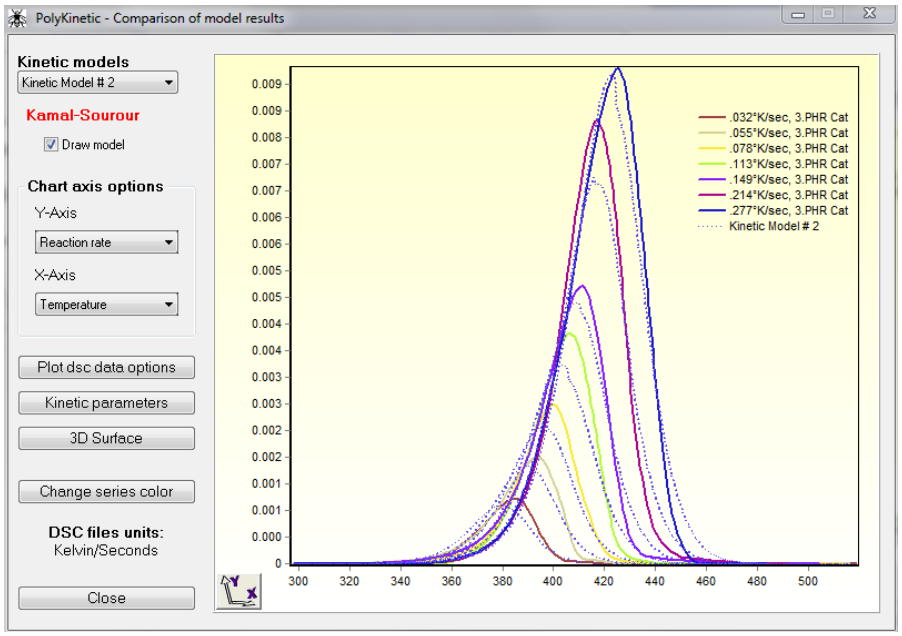

Figure 4. Development of Kamal-Sourour model and comparison of model and experimental results

NUMERICAL SIMULATION AND VALIDATION

TABLE II. THERMAL PROPERTIES FOR MATERIALS IN THE NUMERICAL SIMULATION

	NCF	resin	air
Thermal conductivity (W/mK)	2;0.5;0.5 (1,2,3 dir)	0.11	0.02
Specific heat (J/kg.K)	710	1205	1013
Density (kg/m^3)	1700	1100	1.2

Injection Simulation

Three dimensional solid elements were used to discretize the eight layer NCF square carbon fiber preform. During the finite element mesh discretization important regions such as injection, vent, etc. were defined on the model as exactly used in the experiment. One hexagonal element was used to model each layer of the preform. Table II shows the thermal properties of the preform and the resin used for the simulation. The temperature of the mold was kept uniform at 130 deg. C.

In the simulation, an injection pressure of 40 Psi (0.276 MPa) was used in the experiments. A mean fill time of 55 sec was measured in the injection experiments. At the time of the study, the permeability measurements of the preform were not complete and hence, an inverse method was used to calculate the permeability by matching the fill time with experiments. For inverse analysis, the empirical equations of permeability of uni-directional fabrics in the longitudinal fiber and transverse directions from Gebart [20] was used. Following relations provide the values of permeability of the uni-directional preform, the direction of the fiber K_L and perpendicular to the fiber, K_T.

$$k_L = \frac{8r^2}{c}\frac{(1-V_f)^3}{{V_f}^2}, \quad k_T = C_1\left(\sqrt{V_{fmax}/V_f} - 1\right)^{5/2} r^2 \qquad (14)$$

In the above equation, r denotes the fiber radius, V_f the volume fraction of the preform, V_{fmax} the maximum volume fraction possible for the fiber arrangement (square or hexagonal packing), and C and C_1 are the constants. In this study, a square packing arrangement of fibers was assumed and from Ref [20], the values of C and C_1 and V_{fmax}were obtained as 57, 0.4, and 0.79, respectively. Based on the square

packing assumption, the relations for the k_L and k_T can be written as

$$k_L = \bar{K}\,, \quad k_T = 0.18\,\bar{K} \tag{15}$$

Thus the two unknown values permeability for the uni-directional layer were rewritten in terms of one variable, $\bar{K}$ assuming the square packing of fibers in the preform. Further, the permeability tensor for the entire laminate was determined accounting for individual direction, and flow calculations were made. The values of $\bar{K}$ were iterated such that the fill time from the simulation was made to match the experimental fill time. A fine mesh size of 2 mm was used as experience showed that this mesh can provide a converged solution. Table III shows the permeability values derived from the inverse analysis.

In the above inverse analysis, the channel permeability was assumed as $k_{channel} = 3 \times 10^{-8}$.

A convergence study for the mesh size was conducted to determine the optimum mesh size. Table IV shows the filling time obtained from various mesh sizes. Also, the computational time for completing the analysis with different mesh and number of processors was presented. All the computations were performed with 2.13 GHz memory processors. It can be seen from the Table that a square mesh size of 5 mm in both the direction of the plane of the plate is optimum matching the experimental fill time with a good accuracy and computational efficiency.

TABLE III. PERMEABILITY VALUES DETERMINED FROM INVERSE ANALYSIS FOR THE NCF FABRIC

Layer/Laminate	$K_{X/L}$ (m^2)	$K_{Y/T}$ (m^2)	K_Z(m^2)
0^0 deg. layer (local L and T)	2.95×10^{-11}	5.43×10^{-12}	3×10^{-12}
QI $(0/45/-45/90)_s$- X and Y	1.75×10^{-11}	1.75×10^{-11}	3×10^{-12}

TABLE IV. MESH REFINEMENT STUDY TO CONFIRM THE NUMERICAL CONVERGENCE

Element mesh size (mm)	Number of elements	Computational Time (seconds)			Fill Time (seconds)
		4 CPU	8 CPU	16 CPU	
10x10	117,216	1742	1135	800	57.3
8x8	175,296	3210	2063	1400	57.4
5x5	448,752	12040	7986	3570	56.2
3x3	1,231,104	34670	22131	12278	55.6
2x2	2,775,840	55604	37230	25066	55.2

The pressure profile predicted from the simulation at the inlet sensor with various mesh refinements was presented in figure 5 and one can see that element mesh size of 5 mm provides results very close to results with element size of 2 mm.

Based on the above convergence study, the simulation results with 5 mm mesh are presented in the rest of the paper.

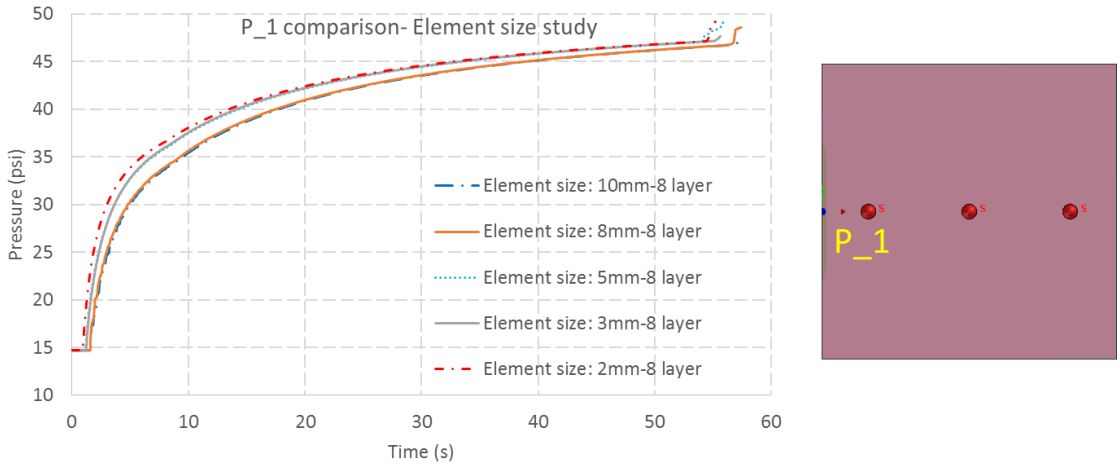

Figure 5. Pressure-time convergence study for different mesh size

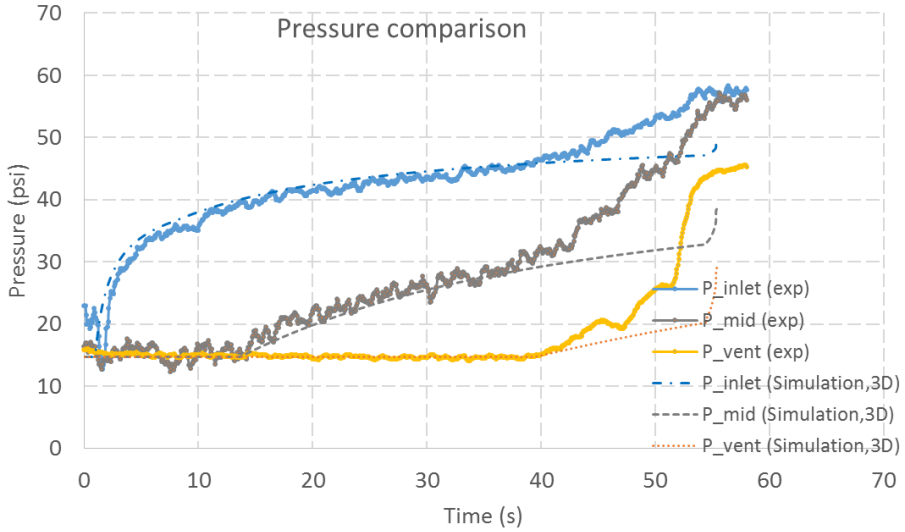

Figure 6. Pressure correlation between 3D RTM simulation and experimental results

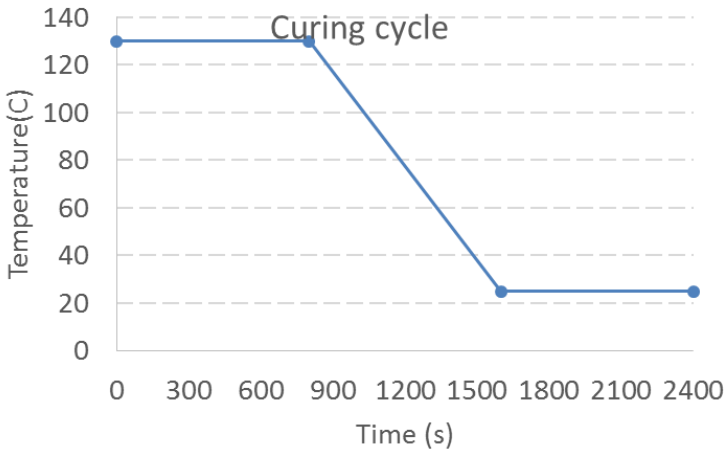

Figure 7. Curing cycle for the experiments and simulations

Validation of Permeability Values:

As the permeability of the preform was calculated inversely matching the fill time, there is a need to validate those permeability values. Towards that, the pressure sensor data from the experiments were correlated with the predicted pressure profiles. Figure 6 shows the variation of pressure with time for the inlet sensor. The predicted pressure profile with time matches closely with the experimental results validating the permeability values for the laminate.

Curing Simulation

Figure 7 shows the curing cycle used for the simulation. The enthalpy of the resin was assumed to be 350,000 J/kg.

The exothermic model implemented was validated by comparing the temperature increase in the preform during the curing. Towards that, two thermocouples were inserted in the mid- plane of the preform and the temperature increase was measured during the resin cure. Figure 8 shows the placement locations of the thermocouple in the mold. They were placed 10 cm away from corners on the vent side of the edge. Figure 8 also shows the comparison between the temperature recorded at the two thermocouple locations and the numerical prediction. One can see from the Figure that the average temperature increase during the exothermic reaction time was predicted very closely with experiments. After the peak temperature rise, the numerical prediction cannot be compared with the experiments as the boundary conditions in the experiment do not match with the simulation boundary conditions (cooling of the mold surfaces after the peak temperature increase was not possible in the experiment to match with the simulation boundary conditions of the fixed 130 deg. temperature at the the top and bottom nodes of the preform.).

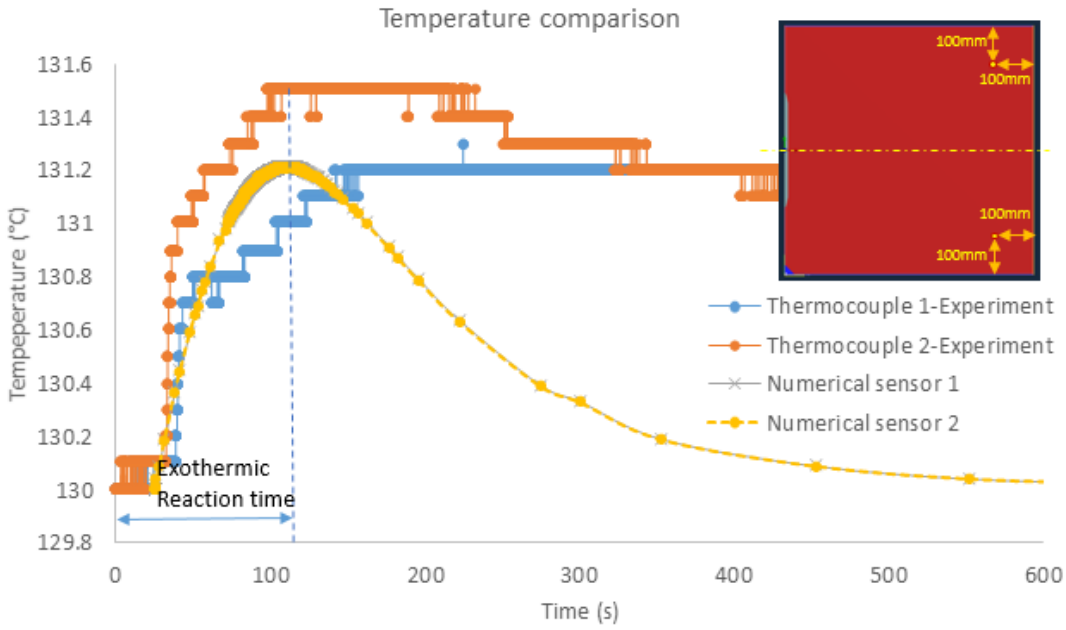

Figure 8. Temperature correlation between 3D Curing simulation and experimental results

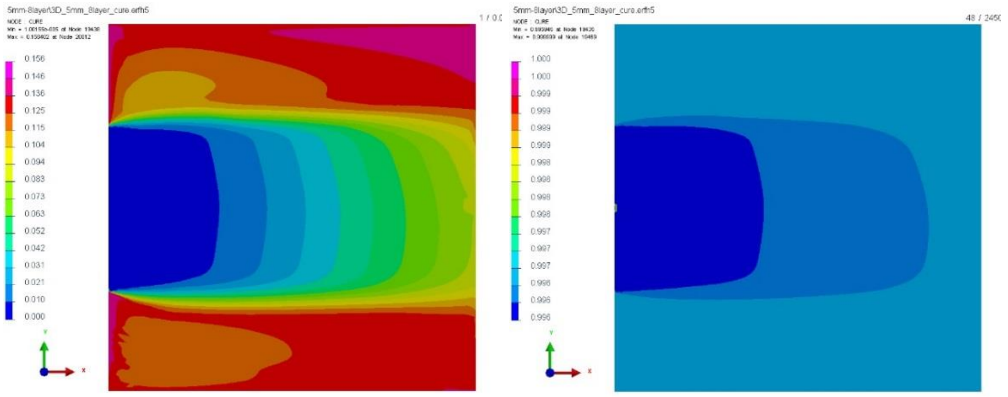

Figure 9. Result of degree of cure after injection (left) and after the hold (900 seconds from the start)

Figure 9 shows the variation of the cure degree after the injection (~55 sec) and after the 900 sec of the start of the process. At the end of injection, a curing degree of 15.6% was achieved. The resin closer to the vent has higher curing degree due to the reason that the resin stays in the mold longer time than the resin near the inlet area.

The degree of cure of the resin was measured using dielectric sensors with time and plotted in Figure 10(a). The units are natural logarithmic of ionic viscosity. The degree of cure predicted from the simulation is shown in Figure 10 (b).

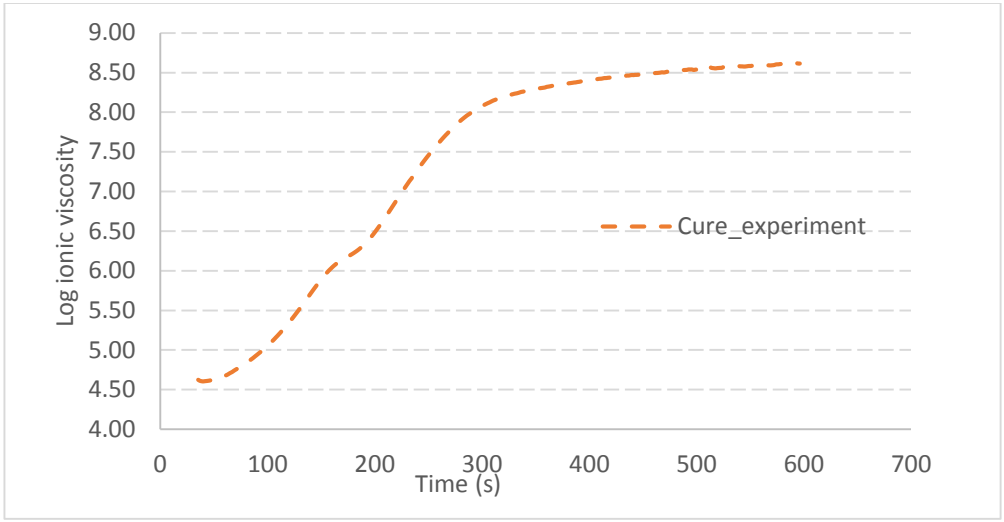

(a)

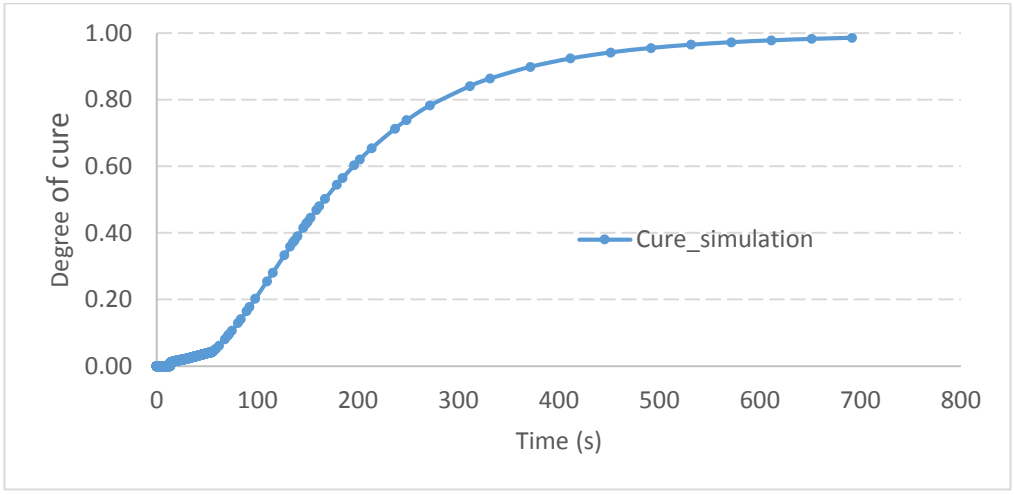

(b)

Figure 10. Cure data of the resin a) ionic viscosity from experiment b) degree of cure from simulation

To compare the curing data available in different units, following assumptions made for the viscosity variation with degree of cure.

$$\mu^{Sim} = a * \left(\frac{1}{T}\right)^{b} \left(\frac{\alpha_g}{\alpha_g - \alpha}\right)^{A+B\alpha} \tag{16}$$

μ^{Sim} is the viscosity calculated from the degree of cure predicted from the simulation. Variables a and b are obtained by calibrating the experimental viscosity with temperature using Equation (4). The unknown terms A and B are calibrated by minimizing the difference between the viscosity calculated and ionic viscosity measured. The equation to solve for the unknown coefficients A, B and the scaling factor C is given as:

$$\min[\ln(\mu^{Sim}) - C * \ln(\mu^{exp})] \text{ for A, B and C} \tag{17}$$

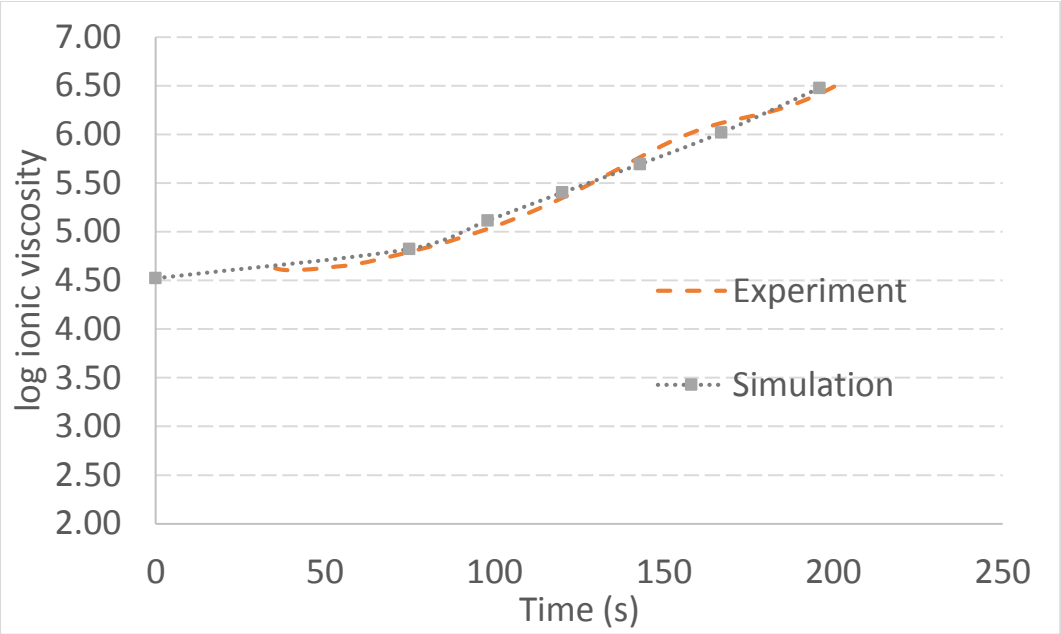

Figure 11. Comparison of viscosity calculated from simulation and experiments.

The scaling constant, C is assumed to relate the viscosity measured from experiments and simulations, respectively. The above equation was solved for A, B and C at few points from the curve in 10 (a). After obtaining the values for A, B, and C, the experimental measurement and simulation derived quantities are compared and observed a good agreement (Figure 11).

Distortion Simulation

The symmetrical laminate considered in the molding study (0/45/-45/90/90/-45/45/0) do not have any coupling between the membrane and bending strain. During the curing/cooling, the molded part does not show significant out of plane displacement as distortion. Due to this reason, a special laminate scheme was developed with the same preform by a) changing the 45/-45 layers of the preform to create an unsymmetrical laminate (0/45/-45/90/90/45/-45/0), and b) rotating 10 degrees the bottom half of the preform to create an unsymmetrical laminate (0/45/-45/90/100/-35/55/10). Table V provides the material properties of the resin during the glassy and rubbery states. The fiber properties are also provided in the Table V. The properties of the composite were calculated using micromechanics equations [26]. Table VI provides the properties of the resin to model the variation of glass transition temperature with the degree of cure

TABLE V. PROPERTIES OF RESIN MATRIX

Property	Resin (glassy)	Resin (rubbery)	Carbon Fiber
Young's Modulus - GPa	2.9	0.033	230 (fiber direction) 15 (transverse direction)
Poisson's ratio	0.3	0.4943	0.2
Shear modulus - GPa	1.115	0.011	15 (in-plane) 4.9 (transverse)
Coeff. of thermal expansion (glassy)	5.5e-5 1/C	1375e-7 1/C	-7.5e-7 1/C (fiber direction) 7 e-6 (transverse direction)
Coeff. of chemical shrinkage (glassy)	-0.005	-0.005	-

TABLE VI. VARIATION OF GLASS TRANSITION TEMPERATURE WITH DEGREE OF CURE (DI BENEDETTO MODEL)

Property	Value
Degree of cure at gelation	0.7
T_{g0}	-50 deg C
$T_{g\infty}$	114.32 deg C
λ	0.8847

The unsymmetrical layups [0/45/-45/90/90/45/-45/0] and [0/45/-45/90/100/-35/55/10] were simulated and the predicted results for the warpage were compared with the experiments. Figure 12 shows the comparison of the warpage from the simulations and experiments for the unsymmetrical lay-up [0/45/-45/90/90/45/-45/0]. The maximum transverse displacement predicted from the simulation is 25.8 mm compared to 20 mm measured in experiments.

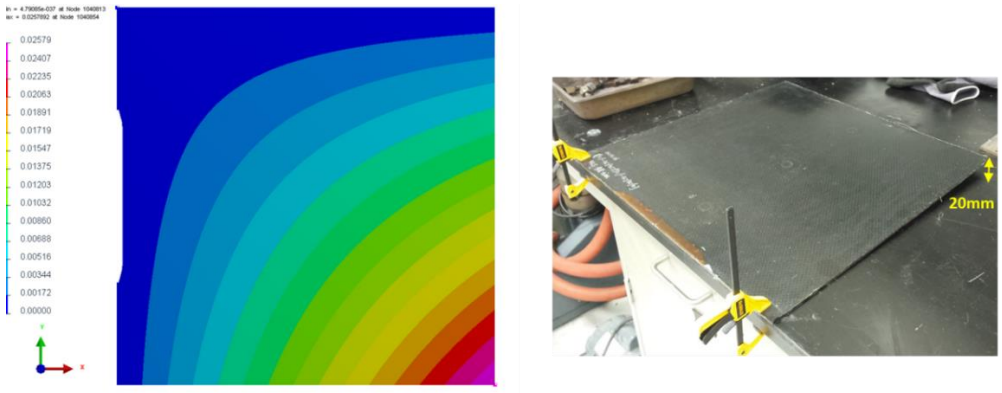

Figure 12. Left: distortion simulation result for the 8-layer unsymmetrical laminate with [0/45/-45/90/90/45/-45/0] layup. The displacement unit is meter; right: the experimental molded and distorted part.

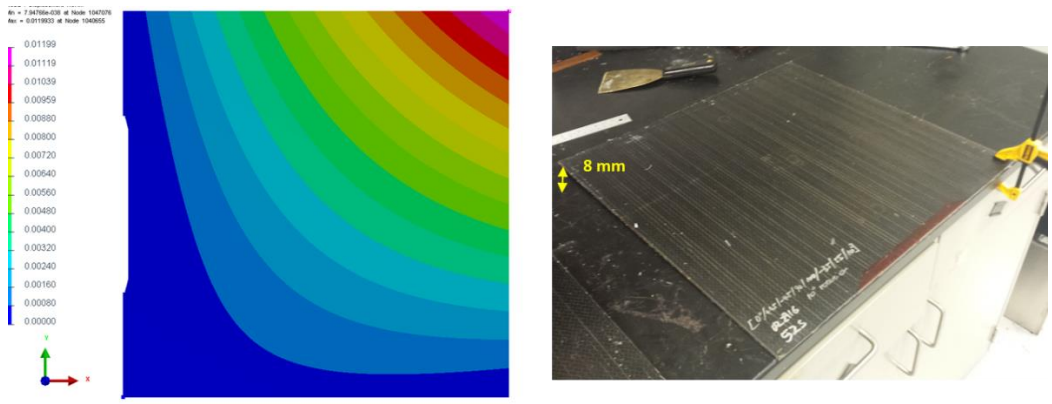

Figure 13. Left: distortion simulation result for the 8-layer unsymmetrical laminate with [0/45/-45/90/100/-35/55/10] layup. The displacement unit is meter; right: the experimental molded and distorted part.

Figure 13 shows the comparison of warpage predicted in the simulation and experiments for the lay-up [0/45/-45/90/100/-35/55/10]. From the figure, we can see that distortion displacement was again over predicted compared with the experiments (11.9 mm with the experimental measurement of 8 mm). The root cause of over prediction of displacement was due to the limitation of the solver available for solving the problem (linear solver considering strain displacement relations to be linear). In the future, plans are in place to implement a full geometrical nonlinear solver for the distortion problem.

CONCLUSIONS

Various stages of resin transfer molding process, such as resin injection, resin curing and part distortion stages were modeled and validated with experimental molding performed at General Motors Research and Development Center. An eight-layer quasi-isotropic NCF carbon fiber preform was selected for the resin injection experiments and two unsymmetrical layup laminates were chosen to compare the distortion of the demolded parts. The results show that the simulation tool was able to provide a good prediction for the fill time, pressure build-up versus time, cure evolution and warpage profile. The study finds that the simulation tool has the potential to design and optimize the resin transfer molding process in order to reduce the manufacturing cost for high volume applications.

ACKNOWLEDGEMENTS

The information, data, or work presented herein was funded in part by the Office of Energy Efficiency and Renewable Energy (EERE), U.S. Department of Energy, under Award Number DE-EE0006826. The information, data, or work presented herein was funded in part by an agency of the United States Government. Neither the United States Government nor any agency thereof, nor any of their employees, makes any warranty, express or implied, or assumes any legal liability or responsibility for

the accuracy, completeness, or usefulness of any information, apparatus, product, or process disclosed, or represents that its use would not infringe privately owned rights. Reference herein to any specific commercial product, process, or service by trade name, trademark, manufacturer, or otherwise does not necessarily constitute or imply its endorsement, recommendation, or favoring by the United States Government or any agency thereof. The views and opinions of authors expressed herein do not necessarily state or reflect those of the United States Government or any agency thereof.

REFERENCES

1. Rudd, C.D., Long, A.C., Kendall, K.N., Mangin, C.G.E., 1997. "Liquid molding technologies, Woodhead Publishing Limited, Cambridge UK.
2. Brooks, N., 1995, *Is RTM ready for mass production*, Reinforced Plastics, Vol 39, No. 1, pp 26-31.
3. Bickerton, S., Advani, S.G., 1997. *Experimental investigation and flow visualization of the resin transfer moldfilling process in a non-planar geometry*, Composites Science and Technology Vol 51, pp 23-33.
4. Lin, M, Hahn, H.T., Huha, H., 1998. *A finite element simulation of resin transfer molding based on partial nodal saturation and implicit time integration*, Composites Part A Vol 29, pp 541-550.
5. Tari, M.J., Imbert, J.P., Lin, M.Y., Lavine, A.S., and Hahn, H.T., 1998. "Analysis of resin transfer molding with high permeability layers", *Journal of Manufacturing Science and Engineering*, Vol 120, pp 609-616.
6. Mohan, R.V., Ngo, N.D, and Tamma, K.K., 1999. *On a pure finite-element-based methodology for resin transfer mold filling simulations*, Polymer Engineering and Science, Vol 39. No. 1. pp 26-43.
7. Lee, D.H., Lee, Woo II, Kang, M.K., 2006. *Analysis and minimization of void formation during resin transfer molding process, Composites Science and Technology*, Vol 66, No. 16, pp 3281-3289.
8. Nguyen, V.H., Deléglise-Lagardère, M., Park, C.H. 2015. *Modeling of resin flow in natural fiber reinforcement for liquid composite molding processes*, Composites Science and Technology, Vol 113, pp 38-45.
9. Bhat, P., Meotte, J., Simacek, P., Advani, S.G., 2009. *Process analysis of compression resin transfer molding", Composites Part A, Applied Science and Manufacturing*, Vol 40, No. 4, pp 431-441.
10. Wang, X., Zhao, Y., Su, H., Jia, Y., 2016. *Curing process-induced internal stress and deformation of fiber reinforced Resin Matrix Composites: Numerical Comparison between Elastic and Viscoelastic Models*, Polymers & polymer composites, Vol 24, No. 2, pp 155-160.
11. Adolf, D. and Martin, J.E. (1996). "Calculation of Stresses in Crosslinking Polymer", *Journal of Composite Materials*, 30(1): 13–34.
12. Eom, Y., Boogh, L., Michaud, V., Sunderland, P. and Manson, J. (2000). *Time-CureTemperature Superposition for the Prediction of Instantaneous Viscoelastic properties during Cure*, Polymer Engineering and Science, 40(6): 1281–1292.
13. J.M. Svanberg and J.A. Holmberg, 2001. *An Experimental Investigation on Mechanisms for Manufacturing Induced Shape Distortions in Homogenous and Balanced Laminates*, Composites: Part A, Vol.32, pp.827-838
14. Shi, F., Dong, X. 2011. *3D numerical simulation of filling and curing processes in non-isothermal RTM process cycle*, Finite Elements in Analysis and Design, Vol 47, Issue 7, pp 764-770.
15. Delegalized, M., Grognec, P., Binetruy, C., Krawczak, P., Claude B. 2011. *Modeling of high speed RTM injection with highly reactive resin with on-line mixing*, Composites Part A: Applied Science and Manufacturing, Vol 42, Issue 10, pp 1390-1397.

16. Ruiz, E., Trochu, F. 2005. *Numerical analysis of cure temperature and internal stresses in thin and thick RTM parts*, Composites Part A: Applied Science and Manufacturing, Vol 36, Issue 6, pp 806-826.
17. Kamal, M.R. and Sourour, S., 1973. "Kinetics and thermal characterization of thermoset cure", Polymer Engineering and Science, 13, 59-64.
18. Svanberg, J. M., and Holmberg, J. Anders, 2004. *Prediction of shape distortions Part I. FE-implementation of a path dependent constitutive model*, Composites Part A: Applied Science and Manufacturing, Vol. 35, Issue 6, Pages 711-721.
19. DiBenedetto A. T., 1987. "Prediction of the glass transition temperature of ploymers: a model based on the principle for corresponding states", *Journal of Polymer Science, Part B: Polymer Physcis*, Vol 25, pp 1949-1969.
20. Gebart, B.R., 1992. "Permeability of unidirectional reinformcements for RTM", *Journal of Composite Materials*, Vol 26, No. 8, pp 1100-1133.
21. Laurent Dufort, Jia Lijie, Wei Ran, Liu Weiping , Yan Dongxiu, 2015. "Prediction of autoclave curing of aeronautical composites parts and of resulting spring-in through esi composites simulation solution, " 20th International Conference on Composite Materials, Copenhagen, 19-24th July 2015.
22. D'Amato, E. 2007. *Numerical modeling and experimental studies for shape and dimensional control in the curing process of textile composites*, Composite Structures, Vol 81, Issue 1, pp 11-20.
23. Abbassi, A., Shahnazari, M.R. 2004. *Numerical modeling of mold filling and curing in non-isothermal RTM process*, Applied Thermal Engineering, Vol 24, Issue 16, pp 2453-2465.
24. Canal, L.P., Benavente, M., Hausmann, M., Michaud, V. 2015. *Process-induced strains in RTM processing of polyurethane/carbon composites*, Composites Part A: Applied Science and Manufacturing, Vol 78, pp 264-273.
25. PAM-RTM 2014 User's Guide & Tutorials, 2014, ESI Group.
26. PAM-DISTORTION 2014 User's Guide, 2014, ESI Group.